Published in final edited form as:
J Immunol. 2011 December 15; 187(12): 6428–6436. doi:10.4049/jimmunol.1101459.

p53 serves as a host antiviral factor that enhances innate and adaptive immune responses to influenza A virus

César Muñoz-Fontela[1,†], **Michael Pazos**[2,†], **Igotz Delgado**[1], **William Murk**[1], **Sathish Kumar Mungamuri**[1], **Sam W. Lee**[6], **Adolfo García-Sastre**[2,3,4], **Thomas M. Moran**[2,5], and **Stuart A. Aaronson**[1,*]

[1]Department of Oncological Sciences, Mount Sinai School of Medicine, One Gustave L. Levy Place, Box 1130, New York, New York 10029, USA

[2]Department of Microbiology, Mount Sinai School of Medicine, One Gustave L. Levy Place, Box 1130, New York, New York 10029, USA

[3]Department of Medicine, Division of Infectious Diseases, Mount Sinai School of Medicine, One Gustave L. Levy Place, Box 1130, New York, New York 10029, USA

[4]Global Health and Emerging Pathogens Institute, Mount Sinai School of Medicine, One Gustave L. Levy Place, Box 1130, New York, New York 10029, USA

[5]Immunology Institute, Mount Sinai School of Medicine, One Gustave L. Levy Place, Box 1130, New York, New York 10029, USA

[6]Cutaneous Biology Research Center, Massachusetts General Hospital and Harvard Medical School, Building 149 13th Street, Charlestown, Massachusetts 02129, USA

Abstract

Several direct target genes of the p53 tumor suppressor have been identified within pathways involved in viral sensing, cytokine production, and inflammation, suggesting a potential role of p53 in antiviral immunity. The increasing need to identify immune factors to devise host-targeted therapies against pandemic influenza A virus (IAV), led us to investigate the role of endogenous wt p53 on the immune response to IAV. We observed that the absence of p53, resulted in delayed cytokine and antiviral gene responses in lung and bone marrow, decreased dendritic cell (DC) activation and reduced IAV-specific $CD8^+$ T cell immunity. Consequently, p53−/− mice showed a more severe IAV-induced disease compared to their wt counterparts. These findings establish that p53 influences the antiviral response to IAV, affecting both innate and adaptive immunity. Thus, in addition to its established functions as a tumor suppressor gene, p53 is serves as an IAV host antiviral factor that might be modulated to improve anti-IAV therapy and vaccines.

Influenza A virus (IAV) poses a global health and economic threat due to the emergence of IAV epidemics and pandemics at random intervals (1). The high rate of viral mutation (antigenic drift) and the putative emergence of reassortant strains (antigenic shift) has raised the need to find host-targeted therapeutic strategies to devise antiviral treatments (2, 3). Current efforts are focused on the identification of host factors with a role in the early inflammatory responses to IAV infection, including toll-like receptors (TLRs) (4), C-type lectins (5), inflammasomes (6) and chemokine receptors (7). However, a possible limitation

*Correspondence: Stuart.Aaronson@mssm.edu. Phone: (212) 659 5400. Fax: (212) 987 2240..
†These authors contributed equally to this work.

Disclosures
The authors declare no competing financial interests.

of such strategies is the fact that these protein families are mainly expressed in the hematopoietic compartment, and not in the epithelial cells of the respiratory tract, which as primary targets of the virus, play a key role in the induction of early cytokine and antiviral gene responses (8).

Recently, we identified a positive feedback loop involving p53-dependent enhancement of IFN signaling through transcriptional upregulation of IFN regulatory factor 9 (IRF9) (9). By doing so, p53 not only promotes the trans-activation of IFN-stimulated genes (ISGs), but also enhances IFN production from virus-infected cells. Other reports indicate that in addition to IRF9, other genes involved in innate immunity are also p53 direct transcriptional targets, including pattern recognition receptors such as TLR3 (10), additional IRFs such as IRF5 (11, 12), antiviral genes such as ISG15 (13) and double stranded RNA (dsRNA)-activated protein kinase R (PKR) (14), and pro-inflammatory chemokines such as monocyte chemoattractant protein 1 (MCP-1) (15). These findings strongly suggest that p53, which is ubiquitously expressed both in the epithelium and the hematopoietic compartment, could play an important role in promoting host antiviral cytokine and antiviral responses to IAV. To test this hypothesis we evaluated the onset of immunity in response to influenza A virus (IAV) in wt and p53−/− mice, by systematic analysis of the events that occur in the lungs, bone marrow and draining mediastial lymph nodes (mLNs) after infection. Our findings indicate that p53 is a key regulator of antiviral immunity to IAV, influencing not only innate but adaptive immunity as well. Thus, p53 modulation could provide a novel strategy in efforts to enhance anti-IAV antiviral therapies and vaccines.

Materials and Methods

Mice infection and virus titration

The p53−/− mouse line B6.129S2-*Trp53*$^{tm1Tyj/J}$ (CD45.2^{+}) was purchased from Jackson Laboratories and bred in the Mount Sinai School of Medicine animal facility, and has been previously described (16). This line has been backcrossed with mice of pure C57BL/6 genetic background for more than 10 generations. Wt BALB/c and B6.SJL-Ptprca Pep3b/BoyJ (CD45.1^{+}) were also purchased from Jackson. Rag2/OT-I mice (B6.129S6-*Rag2*^{tm1Fwa}) were purchased from Taconic Farms. All the experiments described were performed with males between 8-10 weeks of age. Animals were sacrificed according to guidelines of the Institutional Animal Care and Use Committee of Mount Sinai School of Medicine. Experimental infection with mouse-adapted Influenza A/X-31/H3N2 virus was achieved by exposing the mice to aerosolized virus ($10^{7.9}$ virus particles/12 ml PBS for 30 min) in an infection chamber (Glass-Col Corp, Model A4212). For virus titration, the lungs were extracted, homogenized in PBS-gelatin (0.1%) and frozen in dry ice-ethanol for preservation. Virus titers were determined by plaque assay in Madin-Darby canine kidney cells (MDCKs), as described elsewhere. To visualize plaques, cells were fixed with paraformaldehide 4% for 20 min, and permeabilized with 0.2% Triton X-100. Cells were stained with rabbit anti-NP antibodies and HRP-conjugated goat anti-rabbit IgG and then stained with True Blue peroxidase substrate (KPL).

Influenza A/PR8/34 (H1N1) and A/X-31 (H3N2) were propagated in 10-day-old embryonated chicken eggs at 37°C. Influenza ΔNS1 virus has been previously described (17) and was propagated in 8-day-old embryonated chicken eggs at 37°C. PR8-OT-I virus has been previously described (18) and was grown in 10-day-old embryonated chicken eggs at 37°C.

Quantitative reverse transcription-PCR (qRT-PCR) analysis

For qRT-PCR analysis, RNA was isolated from lung tissue or bone marrow flushed from femur and tibiae by TRIzol (Invitrogen) following manufacturer's instructions. Quantitative RT-PCR was performed using 100 ng of sample RNA and SYBR green (Roche) in an ABI PRISM 7900HT instrument following manufacturer's instructions.

OT-I T cell proliferation assay

Mice were infected with PR8-OT-I virus as described above. 2h after infection mice were adoptively transferred with 2×10^6 T cells isolated by negative selection from spleens of naïve Rag2/OT-I mice using magnetic beads and specific antibodies (Miltenyi Biotec). Before adoptive transfer, cells were labeled with 2 mM of carboxyfluorescein succinimidyl ester (CFSE). Cell transfer was accomplished by intravenous (i. v.) injection of cells via retro-orbital sinus. 4 days post-infection mice were sacrificed and ovalbumin (OVA)-specific T cell proliferation was analyzed by flow cytometry. The % of cells divided and the proliferation index was calculated using FlowJo software proliferation platform (Treestar).

In vivo CTL assay

Mice were infected with X-31 virus as described. 8 days after infection, mice were adoptively transferred with splenocytes from congenic donor naïve mice pulsed with OVA-specific H-$2K^b$ - restricted SIINFEKL peptide or an irrelevant peptide. Target cells pulsed with SIINFEKL peptide were labeled with 2.5 mM of CFSE, cells loaded with irrelevant peptide were labeled with 0.25 mM of CFSE. 16 h post-adoptive transfer mice were sacrificed and specific killing of target cells in spleen was analyzed by flow cytometry as previously described (19).

Irradiation and bone marrow transplantation

Eight-week-old recipient mice were lethally irradiated with 1100 rads delivered in two doses of 550 rads each, 4 hr apart. Mice were injected i. v. via the retro-orbital sinus 2h after the second irradiation with 4×10^6 bone marrow cells obtained from wt and p53−/− congenic donor mice (1:1). After transplantation, mice were maintained on antibiotics for two weeks. Hematopoietic engraftment was analyzed by measurement of blood chimerism 4 weeks after transplantation by flow cytometry. Experiments were performed 6 weeks after transplant.

Cell preparation and flow cytometry

Single cell suspensions were obtained from lungs cut into small fragments and digested for 45 min at 37 C with Collagenase D (2mg/ml) (Roche) in RPMI-1640 medium. Single cell suspensions were obtained from mLNs by mechanical disruption without enzymatic digestion. mLNs tissue fragments and digested lungs were further disrupted by passage through a 70-mm nylon cell strainer (BD Biosciences). Red blood cells were lysed with BD Pharm Lyse Buffer (BD Biosciences).

Fc receptors were blocked with CD16/CD32 Fc Block antibody (BD Biosciences) followed by staining with fluorochrome-conjugated antibodies. Fluorochrome-labeled anti-CD86 (GL1), anti-CD103 (Biotin) (2E7), anti-CD8 (53-6.7), and PerCP-Cy5.5-conjugated Streptavidin were from eBioscience. Anti-CD11b (M1/70), anti-Ly6C (AL-21) and anti-CD11c (HL3) were from BD Biosciences. Anti-CD11b (FAB1124F), anti-B220 (FAB1217P) and anti-CD4 (FAB 554F) were from R&D Systems. Anti MHC class II and anti-Ly6C were from Miltenyi Biotec. Anti-MHC class II (M5/114.15.2), anti-CD3 (17A2), anti-F4/80 (BM8), anti-CD45.1 (A20) and anti-CD45.2 (104) were from BioLegend. H-$2K^b$ SIINFEKL pentamer was purchased from Proimmune. Labeling of IAV-specific DCs was accomplished by fixation and permeabilization of single cell suspensions from mLNs using

Cytofix/Cytoperm (BD) following by staining with FITC-conjugated anti-IAV nucleoprotein antibody (Abcam). A FACScalibur or LSR II instrument (BD Biosciences) was used for flow cytometry. Analysis of data was performed with FlowJo software (Treestar).

Influenza virus-specific antibody ELISA

Serum was collected from either naive mice or influenza virus-infected mice on day 9 after infection and examined for influenza virus-specific antibody responses by ELISA. Briefly, 96-well plates were coated overnight at 4°C with 100 μl (10^6 PFU) of heat-inactivated (58°C) A/X-31/H3N2 influenza virus. The plates were washed twice with PBS supplemented with 0.05% Tween-20 (PBST) and blocked with 100 μl of 2% BSA in PBST for 1 h at room temperature. After washing the plates with PBST, 100 μl of diluted serum was added to each well, in duplicate, and incubated for 2 h at room temperature. Bound antibodies were detected by the incubation of horseradish peroxidase-conjugated anti-mouse IgG1 (1:1,000) (BD Pharmingen), IgG2a (R19-15) (1:1,000; BD) and IgG2b (LO-MG2b) (1:1,000) (Southern Biotech) antibodies at room temperature. After 1 h, the plates were washed with PBST, and 100 μl of 3,3′,5,5′-tetramethylbenzidine substrate solution (R&D Systems) was added into each well and incubated for 30 min. The enzyme reaction was stopped by adding 100 μl of 2N H_2SO_4 and OD values were determined at 450 nm using a plate reader (SpectraMax 384 Plus UV-VIS; MDS Analytical Technologies).

Statistical analysis

Statistical significance was evaluated using two-tailed Student's t-test or non-parametric tests (Mann-Whitney), as described for the individual experiments. P values of less than 0.05 were considered statistically significant.

Results

p53 absence causes delayed pulmonary antiviral gene expression after IAV infection

To investigate the influence of the p53 transcriptional program on antiviral responses to IAV, we used quantitative RT-PCR to study IFN-stimulated genes and cytokine profiles in the lungs of wt and p53−/− mice challenged with aerosolized influenza A virus [A/X-31(H3N2)] (IAV). We observed a significantly higher expression of type I IFN-stimulated genes (ISGs), including ISG54, OAS1 and IRF9, at early time points post-infection (day 2) in wt mice infected with IAV compared to p53−/−mice (Fig. 1*A*). These results suggested that p53 promotes the establishment of an IFN-dependent antiviral state in infected lungs. Consistent with this conclusion, wt mice also produced significantly higher amounts of pulmonary IFN-α in response to both A/X - 31/H3N2 and A/PR8/H1N1 virus, as assessed by ELISA (data not shown). Moreover, we observed that p53−/− mice exhibited decreased expression of pro-inflammatory chemokines, including MCP-1, IP-10, MIP-1α, and MIP-1βat day 2 post-infection (Fig. 1*B*). This observation was confirmed at the protein level by analysis of chemokine expression in lungs of infected mice using multiplex ELISA (Supplementary Fig. 1). While wt mice displayed significantly higher mRNA expression levels of pro-inflammatory chemokines and antiviral genes at day 2 post-infection, p53−/− mice exhibited a delayed but significant increase in mRNA transcripts at day 3 post-infection (Fig. 1*B*). To explore whether the known ability of p53 to inhibit viral replication (9, 20) contributed to the observed differences in chemokine kinetics, we evaluated the mRNA levels of IAV nucleoprotein (NP) and non-structural protein 1 (NS1) in the lungs of wt and p53−/− infected mice. Fig. 1*C* shows that, while viral gene expression was similar in wt and p53−/− mice at day 2 post-infection, it was significantly higher in p53−/− mice at day 3 post-infection. Together, these results suggest that, while the rapid innate immune response observed in wt mice was able to maintain low viral titers, in the absence of

functional p53, viral titers peaked at day 3, provoking a later pro-inflammatory response (Fig. *1A-C*).

p53 enhances viral clearance and alleviates IAV-induced disease

To evaluate the biological consequences of p53 absence on IAV-induced disease, we analyzed viral titers in lung homogenates from wt and p53−/− IAV-infected mice by plaque assay. Consistent with our qRT-PCR data, viral titers were significantly higher in p53−/− compared to wt mice at day 3 post-infection (Fig. 2*A*). Moreover, while wt mice were able to clear virus from lungs by day 7 post-infection, there was still detectable virus in the lungs of p53−/− mice at this time point (Fig. 2*A*). These results suggested that the delayed expression of ISGs and chemokines in p53−/− mice impairs their ability to effectively clear virus from the lungs.

To determine the influence of p53 on IAV-associated pathogenesis, we infected wt and p53−/− mice with X-31 and evaluated virus-associated weight loss and pulmonary pathology. We observed that weight loss after X-31 infection was significantly greater in p53−/− mice, which lost 20% of their initial body weight (Fig. 2*B*). These results indicated that the absence of p53 resulted in a more severe IAV-induced morbidity. To rule out viral strain-dependent effects and to test the effect of p53 absence in response to highly pathogenic IAV, we infected wt and p53−/− mice with A/Puerto Rico/8/1934 (H1N1) virus (PR8), and evaluated survival in response to infection. As shown in Fig. 2*C*, p53 deficiency significantly increased mortality in response to PR8 challenge, with only 14.3% of p53−/− mice surviving the infection compared to 42.8% of wt mice (Fig. 2*C*).

Moreover, in agreement with a delayed inflammatory response in the absence of p53, lung sections revealed a robust leukocyte infiltration in wt mice at day 3 post-infection, whereas p53−/− mice did not show any signs of infiltration of immune cells at this time point (Supplementary Fig. 2). Conversely, p53−/− mice exhibited a massive delayed leukocyte infiltration by day 6, as well as severe necrosis of the bronchial epithelium. These observations suggested that the absence of p53 delays the initial innate immune response to IAV, leading to increased IAV-induced disease.

Defective immune response in p53−/− mice impairs bone marrow antiviral instruction and pulmonary monocyte infiltration

Previous studies have demonstrated that lung cytokines produced during IAV infection promote an antiviral state in the sterile, non-infected bone marrow, and enhance migration of leukocytes to the infected lung (21). Thus, to evaluate whether p53 status also affected the establishment of an antiviral state in the bone marrow, we evaluated the expression of antiviral genes and pro-inflammatory chemokines and cytokines in this compartment, in wt and p53−/− IAV-infected mice. Fig. 3*A* shows that at day 2 post-infection, wt mice displayed a significantly higher mRNA induction of antiviral genes than p53−/− mice. At day 3, the overall mRNA levels of antiviral genes was significantly reduced both in wt and p53−/− mice, suggesting that the induction of a IAV-induced antiviral state in the bone marrow, depends to a great extent on the production of early pulmonary cytokines. In any case, at day 3 p53−/− mice showed significantly higher up-regulation of antiviral genes, consistent with the observation of high levels of viral replication in the lungs at this time point (Fig. 3*B*).

Pro-inflammatory chemokines such as MCP-1, IP-10, RANTES, and MIP-1α,prompt the recruitment of leukocytes to sites of inflammation during IAV infection (8). Specifically, MCP-1 and IP-10, which are produced by infected epithelial cells and macrophages/monocytes, have been reported to promote mobilization of bone marrow monocytes as well

as inflammation-dependent pulmonary monocyte infiltration (8). Indeed, during the course of IAV infection, we observed pulmonary infiltration of cells phenotypically characterized by the absence of DC markers ($CD11c^{-}$ MHC II^{-}) and by the expression of monocyte markers ($CD11b^{+}$ $F4/80^{+}$ $Ly6C^{+}$), consistent with migratory blood monocytes (Fig. 4*A*). However, p53−/− mice showed a significantly reduced infiltration of such cells as compared to wt mice (Fig. 4*A*). Taken together, our results indicate that after IAV infection, p53 absence impairs early expression of antiviral genes not only in the lungs, but also in the bone marrow. As a result, p53−/− mice showed less effective pulmonary monocyte infiltration than wt mice.

Defects in monocyte recruitment in p53−/− mice are associated with impaired DC responses

In the lungs, monocytes give rise to the two major populations of myeloid dendritic cells (DCs), $CD103^{+}$ DCs and $CD11b^{+}$ DCs (22, 23). To assess the influence of p53 on the immunobiology of pulmonary DC subsets, we evaluated the kinetics of $CD103^{+}$ DCs and $CD11b^{+}$ DCs in IAV-infected wt and p53−/− mice. Due to the fact that CD11c expression does not distinguish DCs and macrophages in the lungs (22), we gated DCs based on the expression of CD11c, MHC II and side scatter profile, as previously described (24). We identified two main subsets of myeloid DCs, consisting of $CD11c^{+}$ $MHCII^{high}$ $CD11b^{high}$ $CD103^{-}$ $B220^{-}$ DCs ($CD11b^{+}$ DCs) and $CD11c^{+}$ $MHCII^{high}$ $CD11b^{-}$ $CD103^{+}$ $B220^{-}$ DCs ($CD103^{+}$ DCs), which displayed similar steady state frequencies in uninfected wt and p53−/− mice (Fig. 4*B*).

When we compared the kinetics of the response of these DC subsets to IAV infection, we observed a very different dynamic profile for both DC populations. $CD11b^{+}$ DCs accumulated in the lungs of both wt and p53−/− infected mice, whereas $CD103^{+}$ DC numbers decreased early in the course of infection (Fig. 4*B*). These differences in dynamics have been previously reported and are a consequence of greater numbers of $CD103^{+}$ DCs migrating to the draining mediastinal lymph nodes (mLNs) at early time points after infection (25) as well as pulmonary infiltration of $CD11b^{+}$ monocyte-derived DCs (moDCs) (25, 26). Of note, while pulmonary $CD11b^{+}$ DCs accumulated to a greater extent in infected wt mice compared to p53−/− mice, $CD103^{+}$ DCs decreased to a greater extent in wt mice (Fig. 4*B*). These differences are consistent with our observations of reduced monocyte infiltration in p53−/− mice as a result of a defective inflammatory response.

In order to evaluate whether the observed differences in DC kinetics influenced DC migration from lungs to mLNs, we analyzed the presence of migratory lung DCs in the mLNs in wt and p53−/− mice following IAV challenge. Migratory DCs were identified in the mLNs as a population of $CD11c^{med}$ $MHCII^{high}$ cells, as previously described (25). This cell population contained the two main subsets of lung DCs, $CD11b^{+}$ and $CD103^{+}$ DCs. In IAV-infected wt mice, the total accumulation of $CD11c^{+}$ DCs in mLNs was significantly higher than in their p53−/− counterparts (Fig. 4*C*). Further analysis revealed that $CD103^{+}$ DCs arrived at mLNs primarily at early time points after infection (between day 3 and 5), whereas $CD11b^{+}$ DCs accumulated in mLNs at later time points, in agreement with previous reports (25, 27). There was significantly less migration of $CD103^{+}$ DCs in p53−/− mice at day 3 compared to wt mice, as well as significantly less accumulation of $CD11b^{+}$ DCs at all measured time points (Fig. 4*C*).

Effective DC migration to draining lymph nodes relies on their activation status, which in the context of viral infection depends to a great extent on type I IFN signaling (28, 29). To evaluate DC activation defects caused by the absence of p53, we quantified the expression of the activation marker CD86, in pulmonary DC subsets in mock-infected wt and p53−/− mice, or infected with IAV for 6 days. CD86 expression was significantly higher in both

CD11b$^+$ and CD103$^+$ DCs in the presence of wt p53 (Supplementary Fig. 3). To assess whether the influence of p53 in DC maturation was related to its ability to enhance type I IFN signaling, we infected bone marrow-derived DCs (BMDCs) with wt IAV as well as with a recombinant influenza virus lacking the IFN-antagonist protein NS1 (ΔNS1) which *in vitro*, prevents DC maturation by blocking the type I IFN response (28). To determine the maturation/activation status of infected BMDCs, we quantified the expression levels of MHC class II, an *in vitro* maturation marker, by flow cytometry. We observed that the absence of p53 significantly reduced the expression of MHC class II BMDCs infected with ΔNS1 virus, but not with wt IAV, which prevented DC maturation in both wt and p53−/− BMDCs (Supplementary Fig. 3). These results indicated that virus-induced DC activation was impaired in the absence of p53 and that this effect depended at least to some extent on the ability of p53 to enhance type I IFN signaling. Taken together, our findings indicated that the defective induction of antiviral genes and pulmonary monocyte recruitment observed in p53−/− mice, resulted in impaired accumulation of monocyte-derived DCs (moDCs) in the lungs, reduced DC migration to the mLNs, and impaired DC activation.

p53−/− mice show defective antiviral T cell responses

DCs that capture antigens in the peripheral tissues migrate to the mLNs where they activate specific T cell immunity (30). In order to evaluate whether the differences in DC activation and migration observed in wt and p53−/− mice also influenced IAV-specific T cell immunity, we analyzed the ability of wt and p53−/− BMDCs to promote allogeneic T cell proliferation. To do so, we infected wt and p53−/− BMDCs with ΔNS1 virus and co-cultured these cells with naïve T cells isolated from spleens of BALB/c mice. We used a virus without NS1 to enhance the activation of DCs *in vitro*, which otherwise is prevented in the presence of this viral gene (28). Supplementary Fig. 3 shows that after ΔNS1 infection, wt BMDCs were more efficient inducers of T cell proliferation than p53−/− BMDCs, suggesting that the defective activation observed in p53−/− BMDCs inhibited their ability to induce efficient T cell activation. To evaluate whether the differences in T cell activation observed *in vitro* influenced anti-IAV specific T cell immunity *in vivo*, we compared the cytolytic ability of IAV-specific CD8$^+$ T cells from wt and p53−/− mice. To do so, we infected mice with recombinant PR8 IAV harboring MHC class I H-2K^b-restricted ovalbumin (OVA)-derived peptide (SIINFEKL), designated PR8-OT-I. At 8 days post-infection, mice were adoptively transferred with splenocytes isolated from naïve wt donor mice that were pulsed with SIINFEKL peptide or an irrelevant peptide. Cells loaded with SIINFEKL or irrelevant peptide were labeled with different concentrations of the green dye CFSE to allow their identification by flow cytometry (see materials and methods). We observed that specific killing of cells expressing the SIINFEKL peptide was significantly higher in wt mice compared to p53−/− mice, indicating that the absence of p53 function reduces the efficacy of anti-IAV specific T cell immunity **(**Fig. 5*A***)**.

To evaluate the influence of p53 status on the capability of DCs to drive antiviral CD8$^+$ T cell responses, we infected wt and p53−/− mice with PR8-OT-I virus and evaluated OVA-specific CD8$^+$ T cell proliferation. To do so, mice were adoptively transferred with CFSE-labeled T cells isolated from transgenic Rag2/OT-I mice (harboring OVA-specific CD8$^+$ T cells) in the same day of PR8-OT-I challenge. Four days post-infection, mice were sacrificed, and CFSE$^+$ OT-I-specific CD8$^+$ T cells were identified in the mLNs by flow cytometry. We observed that the absence of p53, significantly inhibited OVA-specific CD8$^+$ T cell proliferation (Fig. 5*B*), suggesting that the defects in antiviral innate immunity associated with the absence of p53, ultimately reduced the effectiveness of adaptive T cell immunity. We observed no significant differences in IgG1, IgG2a and IgG2b serum levels between wt and p53−/− mice (Fig. 5*C*), indicating that p53-dependent enhancement of pro-inflammatory responses influences T cell immunity but not antibody responses to IAV.

p53 deficiency in the non-hematopoietic compartment impairs the antiviral response

To dissect the mechanisms by which p53 participates in the antiviral immune response *in vivo*, we next sought to determine the specific contribution of p53 to the antiviral response in the non-hematopoietic vs. the hematopoietic compartment. To do so, we performed mixed bone marrow transplants (50% wt CD45.1$^+$/50% p53−/− CD45.2$^+$) in lethally irradiated mice on a wt or p53−/− background. Of note, analysis of chimerism 4 weeks after transplant indicated that p53−/− bone marrow engrafted significantly better than wt bone marrow (Fig. 6*A*), presumably due to an enhanced resistance to apoptosis. This dominance of p53−/− engraftment was even higher in p53−/− recipients, in which p53−/− hematopoietic cells accounted for up to 80% of blood leukocytes (Fig. 6*A*). To determine whether the observed defects in DC function associated with the absence of p53 resided in the non-hematopoietic or hematopoietic compartments, we next evaluated the migratory properties of IAV-specific DCs in mixed-bone marrow chimeric mice following infection with X-31 virus. To do so, we infected mice with X-31 virus and evaluated the presence of IAV-antigen-specific migratory DCs in the mLNs between days 0 and 6 post-infection. We observed that the arrival of antigen-bearing DCs was significantly higher in wt compared to p53−/− recipient mice, regardless of their phenotype (CD45.1$^+$ (wt) or CD45.2$^+$ (p53−/−)) (Fig. 6*B* and *C*). We also adoptively transferred chimeric mice with CFSE-labeled OT-I T cells after PR8-OT-I challenge. Four days post-infection, mice were sacrificed, and CFSE$^+$ OT-I-specific CD8$^+$ T cells were identified in mLNs by flow cytometry. As shown in Fig. 6*D*, the absence of p53 in the non-hematopoietic compartment significantly inhibited OVA-specific CD8$^+$ T cell proliferation. Taken together, these results suggest that the early innate antiviral response in lung epithelial cells, which are the primary IAV targets, drives a cascade of events that affect DC responses and T cell immunity, and that p53 deficiency in the non-hematopoietic compartment significantly alters both innate and adaptive anti-IAV immunity.

Discussion

Our present study demonstrates that in the innate immune response to pulmonary IAV infection, the absence of p53 severely impairs early expression of antiviral genes and pro-inflammatory chemokines, including p53-direct target genes such as IRF9 (9) and MCP-1 (15). These findings are consistent with a growing body of evidence indicating that the p53-dependent transcriptional program, in addition to its known influence on apoptosis and cell cycle arrest, enhances the expression of key regulators of innate immunity pathways (9, 10, 12, 14). Indeed, a recent study revealed that innate immune responses in the metazoan *C. elegans* are dependent on p53 function (31). All of these findings suggest that the highly conserved nature of p53 among eukaryotes, may rely more on its role in host immunity than in its functions as a tumor suppressor gene.

Previous studies have indicated that p53-dependent apoptosis plays a role in inhibiting viral replication of several viruses *in vitro* including IAV(20). However, the role of apoptosis in the pathogenesis of and the host response to IAV infection *in vivo*, is not fully understood. Our study demonstrates that p53 promotes the expression of antiviral genes and pro-inflammatory chemokines in the bone marrow, which has been previously shown to contribute to the establishment of a systemic antiviral state (21). Replication of low pathogenic IAV in mice is restricted to the respiratory tract (21, 32) and thus, bone marrow cells are not exposed to the virus. This evidence, indicates that the observed p53-dependent effects on antiviral gene induction in the bone marrow, cannot be dependent on its ability to promote virus-induced apoptosis. Thus, our studies suggest that the role of p53 in the antiviral response to IAV *in vivo*, is dependent on its ability to transcriptionally up-regulate pulmonary cytokine production rather than on its pro-apoptotic functions.

The defective cytokine responses in lungs and bone marrow observed in p53−/− mice, were associated with reduced pulmonary monocyte infiltration in comparison to their wt counterparts. These findings are consistent with evidence that production of pro-inflammatory mediators is necessary for leukocyte infiltration at inflammation sites (8, 33, 34). The recent discovery that MCP-1, a known monocyte chemoattractant, is a bona fide p53 target gene (15) also raises the possibility that direct effects of p53 on MCP-1 expression may account to some extent for the differences observed in pulmonary monocyte infiltration. In fact, recent studies indicate that mice knockout for the MCP-1 receptor, CCR2, show defective monocyte migration to inflammation sites (35).

A previous report indicated that p53 deficiency leads to accelerated immunosenescence and accumulation of memory T cells in CBA/N aged mice, an effect that was particularly obvious in mice older than 15 weeks (36). Of note, we used male mice between 8-10 weeks of age in the C57BL/6 background, which showed an entirely normal immune system as assessed by analysis of leukocyte cellularity in bone marrow and spleens of 9 week-old naïve mice (Supplementary Fig. 4). A slight decrease in splenic $CD8^+$ T cells as well as accumulation of bone marrow monocytes was observed in p53−/− mice (Supplementary Fig. 4). These differences are presumably attributable to a deficiency in type I IFN signaling and MCP-1 production in p53−/− mice, since both type I IFN and MCP-1 have been previously shown to regulate peripheral $CD8^+$ T cell maintenance and bone marrow monocyte emigration (35, 37, 38). Further studies are required to evaluate the influence of aging on the ability of p53 to enhance host antiviral immunity.

Pulmonary IAV infection has been shown to promote infiltration of blood monocytes that differentiate into inflammatory $CD11b^+$ moDCs both in lungs (23, 26) and mLNs (39), and that these $CD11b^+$ DCs have full potential to present microbial antigens and stimulate T cell responses (39, 40). Moreover, pulmonary accumulation of monocytes and $CD11b^+$ DCs has been shown to be essential to ensure viral clearance after infection with respiratory viruses by both T cell dependent and independent mechanisms (21, 26). We observed that p53 absence significantly impaired moDC accumulation in the lungs of infected mice, causing increased viral replication and delayed viral clearance. These findings strongly suggest that a rapid production of IFN-stimulated genes and cytokines during the early phase of IAV infection, is needed for an effective control of viral replication, and that p53-dependent transcription is required for this effect.

p53 absence was associated with defective IAV-specific T cell immunity. These findings further suggest that defects associated with the innate antiviral response also ultimately impact the effectiveness of specific T cell antiviral immunity. A previous study by Grayson et al. reported that p53 was not involved in antiviral T cell responses to Lymphocytic choriomeningitis virus (LCMV)(41). However it should be noted that IAV and LCMV induce very different inflammatory responses. Whereas IAV induces inflammation through pathways influenced by p53 status such as RIG-I and TLR3 (6, 42), LCMV has been shown to primarily engage the TLR2-MyD88/Mal pathway (43). In any case, further studies will be required to evaluate the extent to which the impact of p53 on the immune response to IAV may be translatable to other viral infections.

Since p53 status affected CTL but not IAV-specific antibody responses, it is conceivable that helper $CD4^+$ T cell function is not affected by p53 status. This hypothesis is in agreement with recent reports indicating that innate immune responses to several viruses modulate CTL activity without the involvement of $CD4^+$ T cells or cognate antigen stimulation (7, 37, 44, 45).

Our findings demonstrate that the antiviral effects exerted by p53 rely primarily on its functions in non-hematopoietic cells and are likely dependent on its ability to promote more rapid pro-inflammatory and antiviral gene expression. Of note, mixed-bone marrow chimeric mice showed significantly higher engraftment of p53−/− hematopoietic cells compared to wt cells. Although further experiments will be needed to determine the basis for such differences, we hypothesize that apoptotic defects associated with p53 loss of function may provide an advantage in adaptation to the host environment (46, 47). Even though bone marrow-derived p53−/− cells outnumbered wt cells in both wt and p53−/− recipients, we still observed that the absence of p53 in non-hematopoietic cells inhibited migration of DCs carrying IAV antigens to the draining lymph nodes and prevented efficient T cell immunity. These findings strongly suggest that antiviral gene expression and cytokine production in non-hematopoietic cells infected with IAV play a major role in the recruitment of inflammatory cells, the activation of DC functions, and the onset of specific T cell immunity. This may help to explain the multifunctional role of cytokines such as type I IFNs and chemokines such as RANTES or MCP-1, which have been recently shown to fine-tune different aspects of the antiviral adaptive immune response, such as T cell cross-priming (38), peripheral $CD8^+$ T cell maintenance (37), and Th2 polarization (48).

Our present studies strongly support the concept, that enhancement of p53 functions as a host resistance factor against IAV infection, may be used as a host-targeted therapeutic strategy to develop anti-IAV antiviral therapies and vaccine adjuvants. Indeed, recent studies indicate that the enforcement of innate immune responses through the use of TLR ligands, serves to enhance IAV-specific antibody responses (4). These studies strongly suggest that modulation of innate immunity can increase the magnitude and persistence of adaptive immunity. A potential advantage of p53-based therapies in contrast to TLR-directed strategies, is that p53, is expressed by both the epithelial cells primarily infected with IAV, and the immune cell subsets involved in the antiviral response.

Supplementary Material

Refer to Web version on PubMed Central for supplementary material.

Acknowledgments

We thank Rui Qiao and Shen Yao for excellent technical assistance, and Siu-hong Ho and Italas George for assistance at the Flow Cytometry Core Facility, Mount Sinai School of Medicine.

This work was supported by an NIH P01 CA80058-11 grant to S.A.A and partly supported by NIH grants R01 AI046954, U01 AI070469, U19 AI083025, U54 AI057158, and by CRIP, an NIAID supported center for research in influenza pathogenesis, contract number HHS266200700010C to A.G-S, as well as U01 AI082970 and R01 AI41111 grants to T.M.M.

Abbreviations used in this article

IAV	influenza A virus
DC	dendritic cell
TLR	toll-like receptor
IRF	interferon regulatory factor
ISG	interferon-stimulated gene
dsRNA	double-stranded RNA
PKR	double stranded RNA (dsRNA)-activated protein kinase R

MCP-1	monocyte chemoattractant protein 1
MDCK	Madin-Darby canine kidney
NS1	non structural protein 1
NP	nucleoprotein
CFSE	carboxyfluorescein succinimidyl ester
OVA	ovalbumin
mLNs	mediastinal lymph nodes
moDC	monocyte-derived DC
BMDC	bone marrow-derived DC
IP-10	Interferon gamma-induced protein 10 kDa
RANTES	Regulated upon Activation, Normal T-cell Expressed, and Secreted
MIP	Macrophage inflammatory protein

REFERENCES

1. Doherty PC, Turner SJ, Webby RG, Thomas PG. Influenza and the challenge for immunology. Nat Immunol. 2006; 7:449–455. [PubMed: 16622432]
2. Subbarao K, Joseph T. Scientific barriers to developing vaccines against avian influenza viruses. Nat Rev Immunol. 2007; 7:267–278. [PubMed: 17363960]
3. Moss RB, Davey RT, Steigbigel RT, Fang F. Targeting pandemic influenza: a primer on influenza antivirals and drug resistance. J Antimicrob Chemother. 2010; 65:1086–1093. [PubMed: 20375034]
4. Kasturi SP, Skountzou I, Albrecht RA, Koutsonanos D, Hua T, Nakaya HI, Ravindran R, Stewart S, Alam M, Kwissa M, Villinger F, Murthy N, Steel J, Jacob J, Hogan RJ, Garcia-Sastre A, Compans R, Pulendran B. Programming the magnitude and persistence of antibody responses with innate immunity. Nature. 2011; 470:543–547. [PubMed: 21350488]
5. Upham JP, Pickett D, Irimura T, Anders EM, Reading PC. Macrophage receptors for influenza A virus: role of the macrophage galactose-type lectin and mannose receptor in viral entry. J Virol. 2010; 84:3730–3737. [PubMed: 20106926]
6. Ichinohe T, Pang IK, Iwasaki A. Influenza virus activates inflammasomes via its intracellular M2 ion channel. Nat Immunol. 2010; 11:404–410. [PubMed: 20383149]
7. Kohlmeier JE, Miller SC, Smith J, Lu B, Gerard C, Cookenham T, Roberts AD, Woodland DL. The chemokine receptor CCR5 plays a key role in the early memory CD8+ T cell response to respiratory virus infections. Immunity. 2008; 29:101–113. [PubMed: 18617426]
8. Julkunen I, Melen K, Nyqvist M, Pirhonen J, Sareneva T, Matikainen S. Inflammatory responses in influenza A virus infection. Vaccine. 2000; 19(Suppl 1):S32–37. [PubMed: 11163460]
9. Munoz-Fontela C, Macip S, Martinez-Sobrido L, Brown L, Ashour J, Garcia-Sastre A, Lee SW, Aaronson SA. Transcriptional role of p53 in interferon-mediated antiviral immunity. J Exp Med. 2008; 205:1929–1938. [PubMed: 18663127]
10. Taura M, Eguma A, Suico MA, Shuto T, Koga T, Komatsu K, Komune T, Sato T, Saya H, Li JD, Kai H. p53 regulates Toll-like receptor 3 expression and function in human epithelial cell lines. Mol Cell Biol. 2008; 28:6557–6567. [PubMed: 18779317]
11. Yanai H, Chen HM, Inuzuka T, Kondo S, Mak TW, Takaoka A, Honda K, Taniguchi T. Role of IFN regulatory factor 5 transcription factor in antiviral immunity and tumor suppression. Proc Natl Acad Sci U S A. 2007; 104:3402–3407. [PubMed: 17360658]
12. Mori T, Anazawa Y, Iiizumi M, Fukuda S, Nakamura Y, Arakawa H. Identification of the interferon regulatory factor 5 gene (IRF-5) as a direct target for p53. Oncogene. 2002; 21:2914–2918. [PubMed: 11973653]

13. Hummer BT, Li XL, Hassel BA. Role for p53 in gene induction by double-stranded RNA. J Virol. 2001; 75:7774–7777. [PubMed: 11462054]
14. Yoon CH, Lee ES, Lim DS, Bae YS. PKR, a p53 target gene, plays a crucial role in the tumor-suppressor function of p53. Proc Natl Acad Sci U S A. 2009; 106:7852–7857. [PubMed: 19416861]
15. Hacke K, Rincon-Orozco B, Buchwalter G, Siehler SY, Wasylyk B, Wiesmuller L, Rosl F. Regulation of MCP-1 chemokine transcription by p53. Mol Cancer. 2010; 9:82. [PubMed: 20406462]
16. Jacks T, Remington L, Williams BO, Schmitt EM, Halachmi S, Bronson RT, Weinberg RA. Tumor spectrum analysis in p53-mutant mice. Curr Biol. 1994; 4:1–7. [PubMed: 7922305]
17. Garcia-Sastre A, Egorov A, Matassov D, Brandt S, Levy DE, Durbin JE, Palese P, Muster T. Influenza A virus lacking the NS1 gene replicates in interferon-deficient systems. Virology. 1998; 252:324–330. [PubMed: 9878611]
18. Jenkins MR, Webby R, Doherty PC, Turner SJ. Addition of a prominent epitope affects influenza A virus-specific CD8+ T cell immunodominance hierarchies when antigen is limiting. J Immunol. 2006; 177:2917–2925. [PubMed: 16920927]
19. Byers AM, Kemball CC, Moser JM, Lukacher AE. Cutting edge: rapid in vivo CTL activity by polyoma virus-specific effector and memory CD8+ T cells. J Immunol. 2003; 171:17–21. [PubMed: 12816977]
20. Turpin E, Luke K, Jones J, Tumpey T, Konan K, Schultz-Cherry S. Influenza virus infection increases p53 activity: role of p53 in cell death and viral replication. J Virol. 2005; 79:8802–8811. [PubMed: 15994774]
21. Hermesh T, Moltedo B, Moran TM, Lopez CB. Antiviral instruction of bone marrow leukocytes during respiratory viral infections. Cell Host Microbe. 2010; 7:343–353. [PubMed: 20478536]
22. Jakubzick C, Tacke F, Ginhoux F, Wagers AJ, van Rooijen N, Mack M, Merad M, Randolph GJ. Blood monocyte subsets differentially give rise to CD103+ and CD103-pulmonary dendritic cell populations. J Immunol. 2008; 180:3019–3027. [PubMed: 18292524]
23. Lin KL, Suzuki Y, Nakano H, Ramsburg E, Gunn MD. CCR2+ monocyte-derived dendritic cells and exudate macrophages produce influenza-induced pulmonary immune pathology and mortality. J Immunol. 2008; 180:2562–2572. [PubMed: 18250467]
24. Jakubzick C, Randolph GJ. Methods to study pulmonary dendritic cell migration. Methods Mol Biol. 2010; 595:371–382. [PubMed: 19941125]
25. Ballesteros-Tato A, Leon B, Lund FE, Randall TD. Temporal changes in dendritic cell subsets, cross-priming and costimulation via CD70 control CD8(+) T cell responses to influenza. Nat Immunol. 2010; 11:216–224. [PubMed: 20098442]
26. Aldridge JR Jr. Moseley CE, Boltz DA, Negovetich NJ, Reynolds C, Franks J, Brown SA, Doherty PC, Webster RG, Thomas PG. TNF/iNOS-producing dendritic cells are the necessary evil of lethal influenza virus infection. Proc Natl Acad Sci U S A. 2009; 106:5306–5311. [PubMed: 19279209]
27. GeurtsvanKessel CH, Willart MA, van Rijt LS, Muskens F, Kool M, Baas C, Thielemans K, Bennett C, Clausen BE, Hoogsteden HC, Osterhaus AD, Rimmelzwaan GF, Lambrecht BN. Clearance of influenza virus from the lung depends on migratory langerin+CD11b-but not plasmacytoid dendritic cells. J Exp Med. 2008; 205:1621–1634. [PubMed: 18591406]
28. Fernandez-Sesma A, Marukian S, Ebersole BJ, Kaminski D, Park MS, Yuen T, Sealfon SC, Garcia-Sastre A, Moran TM. Influenza virus evades innate and adaptive immunity via the NS1 protein. J Virol. 2006; 80:6295–6304. [PubMed: 16775317]
29. Honda K, Sakaguchi S, Nakajima C, Watanabe A, Yanai H, Matsumoto M, Ohteki T, Kaisho T, Takaoka A, Akira S, Seya T, Taniguchi T. Selective contribution of IFN-alpha/beta signaling to the maturation of dendritic cells induced by double-stranded RNA or viral infection. Proc Natl Acad Sci U S A. 2003; 100:10872–10877. [PubMed: 12960379]
30. Banchereau J, Steinman RM. Dendritic cells and the control of immunity. Nature. 1998; 392:245–252. [PubMed: 9521319]
31. Fuhrman LE, Goel AK, Smith J, Shianna KV, Aballay A. Nucleolar proteins suppress Caenorhabditis elegans innate immunity by inhibiting p53/CEP-1. PLoS Genet. 2009; 5:e1000657. [PubMed: 19763173]

32. Moltedo B, Lopez CB, Pazos M, Becker MI, Hermesh T, Moran TM. Cutting edge: stealth influenza virus replication precedes the initiation of adaptive immunity. J Immunol. 2009; 183:3569–3573. [PubMed: 19717515]
33. Julkunen I, Sareneva T, Pirhonen J, Ronni T, Melen K, Matikainen S. Molecular pathogenesis of influenza A virus infection and virus-induced regulation of cytokine gene expression. Cytokine Growth Factor Rev. 2001; 12:171–180. [PubMed: 11325600]
34. Sladkova T, Kostolansky F. The role of cytokines in the immune response to influenza A virus infection. Acta Virol. 2006; 50:151–162. [PubMed: 17131933]
35. Serbina NV, Pamer EG. Monocyte emigration from bone marrow during bacterial infection requires signals mediated by chemokine receptor CCR2. Nat Immunol. 2006; 7:311–317. [PubMed: 16462739]
36. Ohkusu-Tsukada K, Tsukada T, Isobe K. Accelerated development and aging of the immune system in p53-deficient mice. J Immunol. 1999; 163:1966–1972. [PubMed: 10438933]
37. Kohlmeier JE, Cookenham T, Roberts AD, Miller SC, Woodland DL. Type I interferons regulate cytolytic activity of memory CD8(+) T cells in the lung airways during respiratory virus challenge. Immunity. 2010; 33:96–105. [PubMed: 20637658]
38. Le Bon A, Etchart N, Rossmann C, Ashton M, Hou S, Gewert D, Borrow P, Tough DF. Cross-priming of CD8+ T cells stimulated by virus-induced type I interferon. Nat Immunol. 2003; 4:1009–1015. [PubMed: 14502286]
39. Nakano H, Lin KL, Yanagita M, Charbonneau C, Cook DN, Kakiuchi T, Gunn MD. Blood-derived inflammatory dendritic cells in lymph nodes stimulate acute T helper type 1 immune responses. Nat Immunol. 2009; 10:394–402. [PubMed: 19252492]
40. Cheong C, Matos I, Choi JH, Dandamudi DB, Shrestha E, Longhi MP, Jeffrey KL, Anthony RM, Kluger C, Nchinda G, Koh H, Rodriguez A, Idoyaga J, Pack M, Velinzon K, Park CG, Steinman RM. Microbial Stimulation Fully Differentiates Monocytes to DC-SIGN/CD209(+) Dendritic Cells for Immune T Cell Areas. Cell. 2010; 143:416–429. [PubMed: 21029863]
41. Grayson JM, Lanier JG, Altman JD, Ahmed R. The role of p53 in regulating antiviral T cell responses. J Immunol. 2001; 167:1333–1337. [PubMed: 11466350]
42. Le Goffic R, Pothlichet J, Vitour D, Fujita T, Meurs E, Chignard M, Si-Tahar M. Cutting Edge: Influenza A virus activates TLR3-dependent inflammatory and RIG-I-dependent antiviral responses in human lung epithelial cells. J Immunol. 2007; 178:3368–3372. [PubMed: 17339430]
43. Zhou S, Halle A, Kurt-Jones EA, Cerny AM, Porpiglia E, Rogers M, Golenbock DT, Finberg RW. Lymphocytic choriomeningitis virus (LCMV) infection of CNS glial cells results in TLR2-MyD88/Mal-dependent inflammatory responses. J Neuroimmunol. 2008; 194:70–82. [PubMed: 18295350]
44. Mathew A, O'Bryan J, Marshall W, Kotwal GJ, Terajima M, Green S, Rothman AL, Ennis FA. Robust intrapulmonary CD8 T cell responses and protection with an attenuated N1L deleted vaccinia virus. PLoS One. 2008; 3:e3323. [PubMed: 18830408]
45. Battegay M, Moskophidis D, Waldner H, Brundler MA, Fung-Leung WP, Mak TW, Hengartner H, Zinkernagel RM. Impairment and delay of neutralizing antiviral antibody responses by virus-specific cytotoxic T cells. J Immunol. 1993; 151:5408–5415. [PubMed: 7693811]
46. Benkerrou M, Le Deist F, de Villartay JP, Caillat-Zucman S, Rieux-Laucat F, Jabado N, Cavazzana-Calvo M, Fischer A. Correction of Fas (CD95) deficiency by haploidentical bone marrow transplantation. Eur J Immunol. 1997; 27:2043–2047. [PubMed: 9295043]
47. Bittencourt MC, Perruche S, Contassot E, Fresnay S, Baron MH, Angonin R, Aubin F, Herve P, Tiberghien P, Saas P. Intravenous injection of apoptotic leukocytes enhances bone marrow engraftment across major histocompatibility barriers. Blood. 2001; 98:224–230. [PubMed: 11418484]
48. Gu L, Tseng S, Horner RM, Tam C, Loda M, Rollins BJ. Control of TH2 polarization by the chemokine monocyte chemoattractant protein-1. Nature. 2000; 404:407–411. [PubMed: 10746730]

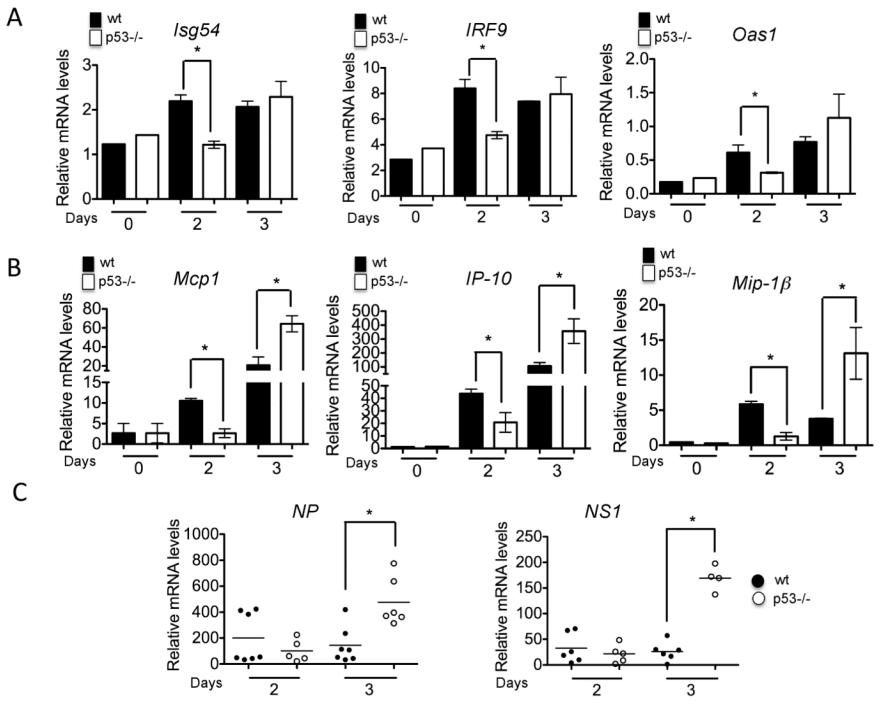

FIGURE 1.

Expression of antiviral genes and pro-inflammatory cytokines in IAV-infected wt (black bars) and p53 mice (white bars). *A*, Quantitative real time PCR for the indicated antiviral genes. RNA samples were obtained from lung tissue of infected mice at the indicated time points and used as a template for qRT-PCR. Results represent the average gene induction in three independent lung samples and are representative of two independent experiments. Results are shown as Mean ± SEM. *B*, qRT-PCR data for the indicated chemokines, as described above. Asterisks represent statistical significance ($p<0.05$), as assessed by student's T test. *C*, Evaluation of IAV nucleoprotein (NP) and non-structural protein 1 (NS1) gene expression in lung samples of wt (black symbols) and p53−/− mice (white symbols) infected with IAV. At least 5 mice were used for each of the indicated time points. RNA samples were obtained from lung tissue and used as template for qRT-PCR analysis. Asterisks denote statistical significance ($p<0.05$), as assessed by Mann-Whitney non-parametric test.

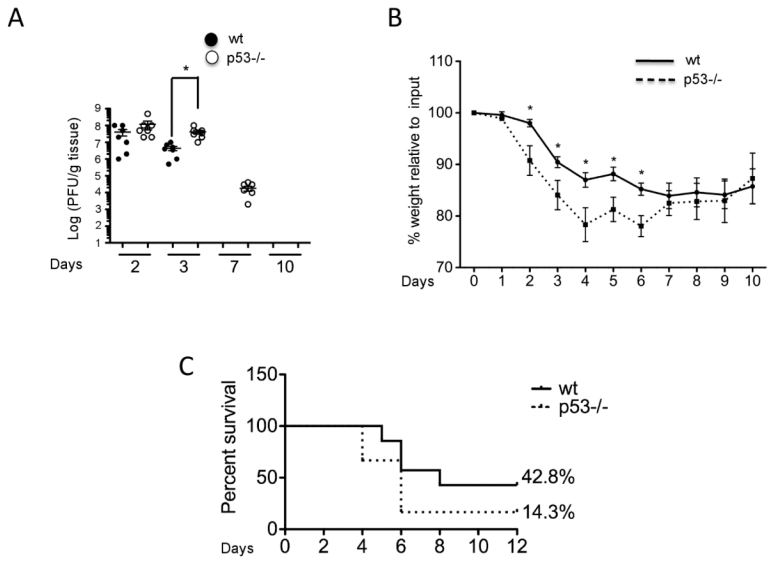

FIGURE 2.

Viral replication and pathogenesis. *A*, Quantification of viral titers by plaque assay followed by immunostaining of plaques using anti-influenza NP antibodies. Lungs from mice infected at the indicated time points were harvested and mechanically homogenized. Lung supernatants were disposed in ten-fold dilutions in 6-well plates seeded with 100% confluent Madin-Darby canine kidney (MDCK) cells for 60 min at room temperature and covered with an overlay of 2% agar for 48 hours. Cells were fixed with 4% paraformaldehide and permeabilized with 0.2% of Triton X-100. Immunostaining of viral plaques was performed as described in experimental procedures. *B*, Analysis of weight loss in wt (unbroken line) and p53−/− mice (dotted line). The numbers in the x axis represent days post-infection. 10 mice of each genotype were used for the assay and results are represented as % of weight loss relative to initial weight. Results are represented as Mean ± SEM. Asterisks represent statistical significance ($p<0.05$) as assessed by student's T test. *C*, Survival in response to A/Puerto Rico/8/1934 (H1N1) infection. Mice were infected intranasally with 1000 pfu of PR8 virus under isoflurane anesthesia. Weight loss and body score were assessed daily, and mice were euthanized if their body weight dropped more than 25% from the initial weight, as per institutional guidelines.

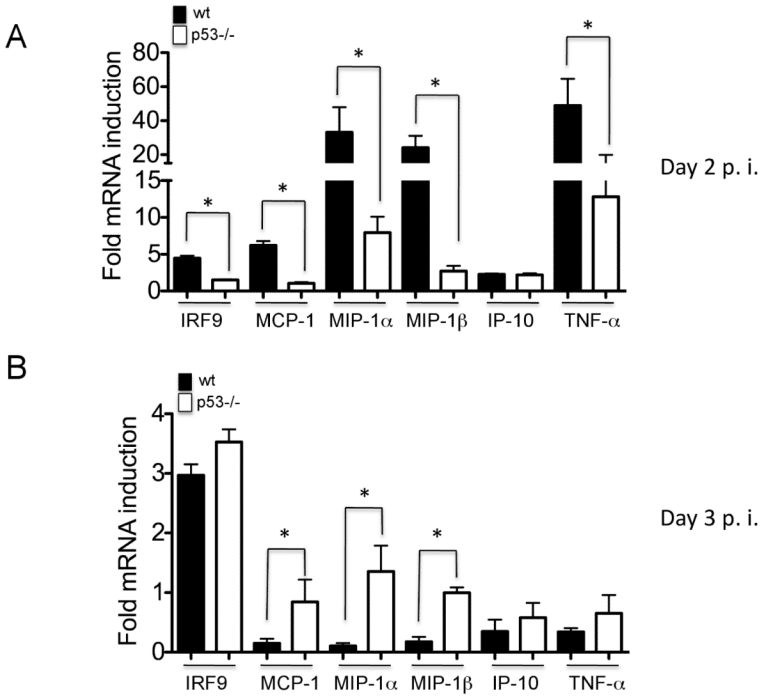

FIGURE 3.

Expression of antiviral genes in the bone marrow. *A-B*, Quantitative real time PCR for the indicated antiviral genes. RNA samples were obtained from bone marrow flushed from femurs and tibiae of infected mice at the indicated time points, and used as a template for qRT-PCR. Results represent the average gene induction in three independent bone marrow samples. Results are shown as Mean ± SEM.

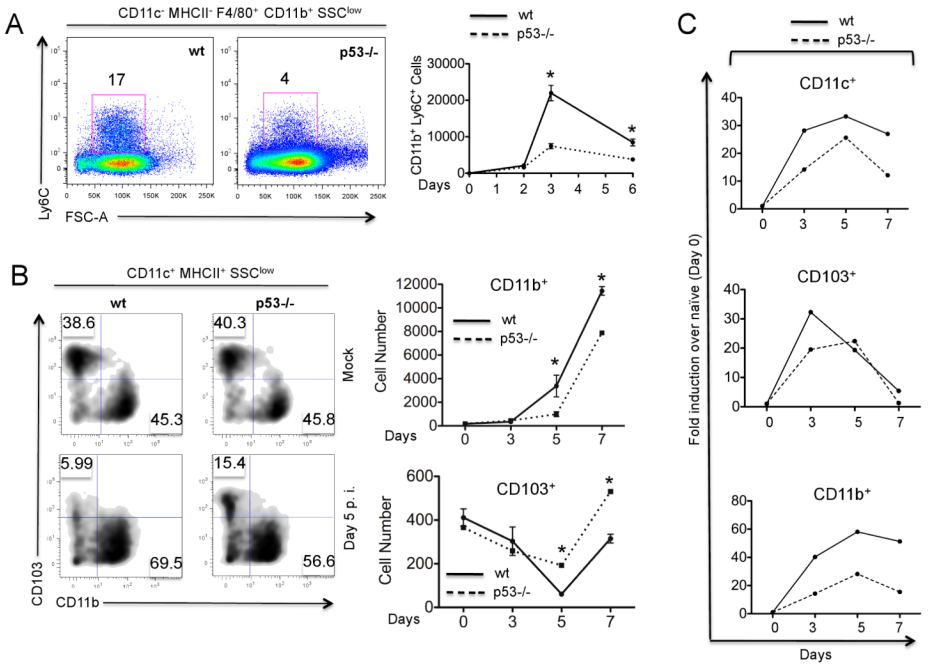

FIGURE 4.

Monocyte infiltration and dendritic cell kinetics in lungs and mLNs. *A*, Flow cytometry analysis of monocyte infiltration in lungs of wt and p53−/− mice infected with IAV for 6 days (left panel) or in a time course (right panel). Monocytes were gated as $CD11c^{-}$ $MHCII^{-}$ $F4/80^{+}$ $CD11b^{+}$ $Ly6C^{+}$ cells in the low side scatter (SSC). Single cell suspensions were obtained from lungs of wt (full line) and p53−/− mice (dotted line) and subjected to FACS analysis as described on the Methods section. Lungs were pooled from three different mice for each time point. In the right panel, results are represented as absolute number of monocytes per 2×10^{5} events in lungs of infected mice at the indicated time points. *B*, Flow cytometry analysis of the kinetics of myeloid DCs in the lungs of wt (unbroken line) and p53−/− mice (dotted line) upon IAV infection. DCs were gated as $CD11c^{+}$ MHC II^{+} cells in the low SSC, and were further defined as $CD103^{+}$ $CD11b^{-}$ $B220^{-}$ ($CD103^{+}$) and $CD103^{-}$ $CD11b^{+}$ $B220^{-}$ ($CD11b^{+}$). In the right panel, numbers on the x axis represent days post-infection and are represented as Mean ± SEM of two independent experiments. *C*, Flow cytometry analysis of DC migration from lungs to draining mLNs. Tissue DCs in the mLNs were defined as $CD11c^{+}$ MHC II^{med} cells expressing either CD11b or CD103. Each point (black for wt and white for p53−/−) represents the average DC numbers in mLNs pooled from three different mice.

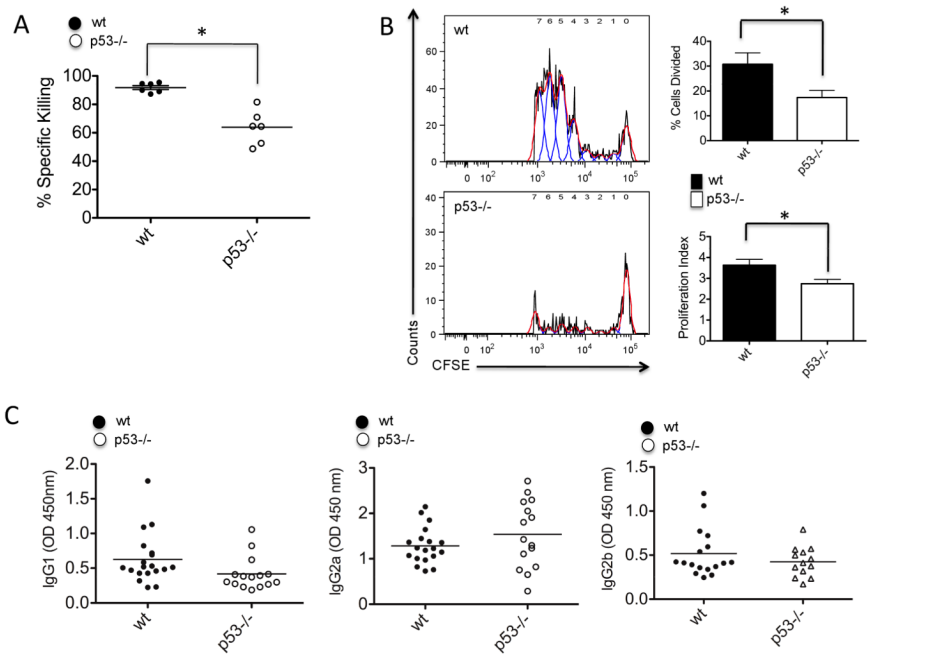

FIGURE 5.

T cell responses in wt and p53−/− mice infected with IAV. *A*, CTL in vivo assay. Wt and p53−/− mice mock-infected with PBS or infected with PR8-OT-I virus for 8 days were adoptively transferred with splenocytes isolated from wt donor mice and pulsed with SIINFEKL peptide or irrelevant control peptide for 60 min. SIINFEKL positive cells and control peptide positive cells were labeled with high vs low CFSE respectively and analyzed by flow cytometry. Analysis of specific killing was done as described in Materials and Methods. *B*, OT-I T cell proliferation. Mice were infected with PR8-OT-I virus and adoptively transferred with CFSE-labeled T cells isolated from Rag2/OT-I mice. At day 4 post-infection, mice were sacrificed and mLNs extracted and prepared for flow cytometry. Left panel represents T cell proliferation as assessed by CFSE dilution. The red line represents the histogram profiles and the blue lines the peaks of proliferation detected using FlowJo's proliferation platform. The panels on the right represent % of cells divided from the parent population of $CD8^+$ T cells, and the proliferation index (average of divisions of each population). These parameters were determined using FlowJo's proliferation platform. *C*, ELISA analysis of IAV specific IgG isotypes in serum 10 days after IAV infection. At least 10 mice were used for the analysis. Serum samples were collected as described in the Methods section and subjected to evaluation in X-31 activated ELISA plates. Results are representative of two independent experiments.

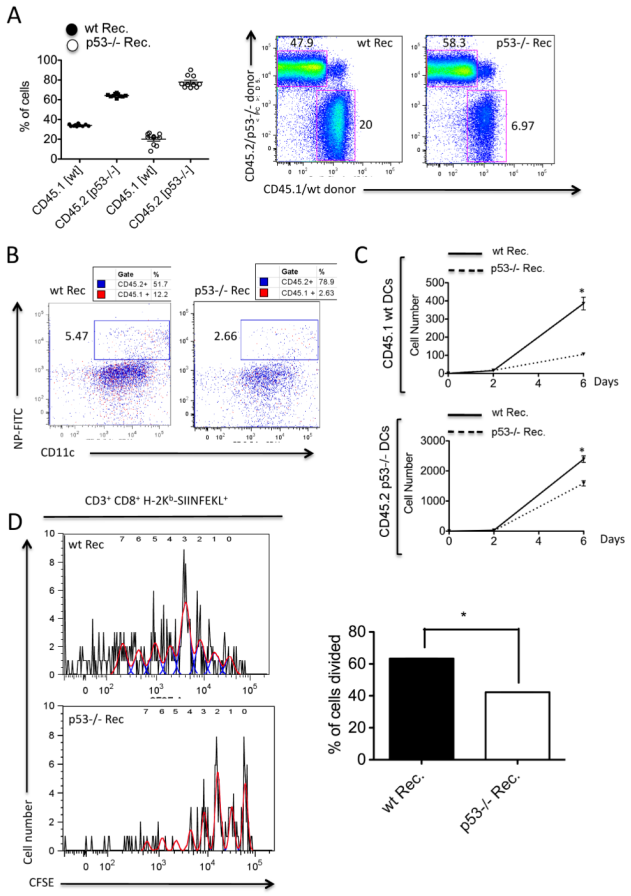

FIGURE 6.

Antiviral responses in mixed bone marrow chimeric mice. *A*, Generation of mixed chimeras. Bone marrow cells from WT and *p53−/−* mice (expressing *CD45.1 and CD45.2*, respectively; 2×10^6 cells from each) were mixed in a 1:1 ratio and transplanted into lethally irradiated congenic WT or p53−/− recipients (expressing *CD45.2*). Engraftment was evaluated 4 weeks after transplant by flow cytometry analysis of CD45.1 and CD45.2 cells in blood. Right panel shows a representative dot plot indicating the contribution of WT and *p53−/−* cells to hematopoietic cells in the mLNs. *B*, Analysis of IAV-specific DCs in the mLNs of wt and p53−/− recipients. Dot plot shows representative data of IAV-specific DCs both in the CD45.1 (wt) and CD45.2 (p53−/−) background. DCs were gated as $CD11c^+$ MHC II^{med} expressing either CD45.1 (red) or CD45.2 (blue). Right panel indicates absolute numbers of IAV-specific DCs per 2×10^5 events. *C*, OT-I T cell proliferation assay. Wt and p53−/− recipient mice were infected with PR8-OT-I virus and adoptively transferred with CFSE-labeled T cells isolated from Rag2/OT-I mice. At day 4 post-infection, mice were sacrificed and mLNs extracted and prepared for flow cytometry. Left panel indicates T cell proliferation as assessed by CFSE dilution. The red line shows the histogram profiles and the blue lines the peaks of proliferation detected using FlowJo's proliferation platform. The panels on the right indicate % of cells divided from the parent population of $CD8^+$ T cells.